

Analysis of Finite Microstrip Structures using an Efficient Implementation of the Integral Equation Technique

Fernando Quesada Pereira and Alejandro Alvarez Melcón

Abstract— An efficient numerical implementation of the Integral Equation technique (IE) has been developed for the analysis of the electrical characteristics of finite microstrip structures. The technique formulates a volume version of the IE for the finite dielectric objects. The numerical implementation combines rooftop basis and testing functions for the conducting metallic areas, and two different choices for the dielectric objects. The first is based on a classical approach, combining pulse basis functions and deltas for testing. The second is a novel full Galerkin approach which employs rooftop functions defined on brick cells inside the dielectrics. The input impedances of two microstrip antennas have been computed with the new technique, showing good agreement with respect measurements. Also the radiation patterns of the antennas have been evaluated, showing again good agreement with respect measurements. The practical value of the approach is that microstrip circuits can be designed minimizing the volume and size of the dielectric substrates. In addition, it is possible to accurately predict the backward radiation of practical microstrip radiators.

I. INTRODUCTION

The study of microstrip structures is a subject that is attracting much attention in microwave engineering, specially for their mechanical advantages and for the integration capabilities with other Radiofrequency circuits offered by these configurations [1].

For the analysis of microstrip structures, the Integral Equation (IE) technique in combination with the multi-layered media Green's functions formulated both in the spectral [2] and in the spatial [3] domain, has grown in popularity. Using this approach, the information of the dielectric layers is included in the Green's functions, so that the numerical treatment of the problem is reduced to the metallic areas printed on the substrates, thus considerably increasing the efficiency of the technique. A big limitation of this approach is that the dielectric layers are considered to be of infinite transverse dimensions [3]. The practical circuits, however, must be of finite size. In order to obtain accurate results with respect the infinite model, the size of the substrates must contain several wavelengths of the circuit, therefore approaching the ideal infinite size situation. A drawback of this design procedure is that the size and volume of the total circuit can not be conveniently

optimized, which might not be acceptable in many satellite and space applications. In addition, the infinite size analysis can not extract other important information such as the backside radiation of printed microstrip antennas [4]. Finally, a third limitation of this technique is that, while the analysis of strictly planar geometries is relatively easy [4], the same is generally not true when vertical or arbitrarily oriented metalizations are included inside the dielectric layers [3], [5].

The techniques that are readily available for the analysis of full 3D finite microstrip structures are the finite elements, finite differences, or the method of lines. These techniques, however, require very intensive numerical computations, specially because the whole volume around the structure must be discretized, often in combination of some sort of absorbing boundary condition [6]. As regards the integral equation technique, some previous attempts for the analysis of finite microstrip structures have been reported, both using volume and surface equivalent formulations [7], [8]. However, only very preliminary results of very simple structures have been presented in [8]. Also in [8] the radiation patterns obtained with volume and surface formulations appear not to agree well, thus indicating limited accuracy in the presented results. In addition, to the authors knowledge no precise investigation of the input impedance of microstrip structures has ever been reported in the literature.

In this contribution we present two efficient numerical implementations of the volume equivalent integral equation technique applied to the analysis of finite microstrip structures. The technique combines rooftop basis and testing functions for the conductor areas with two different choices for the finite dielectric objects. The first is based on combining pulse basis functions and deltas for testing, in a similar way as presented in [8]. Unlike the technique in [8], however, the use of rooftop basis and testing functions for the conductor areas increases the numerical stability of the method, and accurate results are shown to be obtained, both for the input impedance and for the radiation patterns of microstrip antennas. The second choice to treat the finite dielectric objects is a full Galerkin approach, which employs rooftop basis and testing functions defined in the volume of the brick cells used in the discretization of the dielectrics. The advantage of this second formulation is that the derivatives on the scalar potential Green's

Technical University of Cartagena. Campus Muralla del Mar, s/n, E-30202 Cartagena. E-mail: fernando.quesada@upct.es

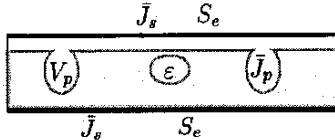


Fig. 1. General finite size microstrip structure analyzed in this paper.

functions are avoided, therefore reducing considerably the level of singularity in the subsequent integration process.

In this contribution, results obtained with both approaches are shown to be accurate, both for the input impedance of microstrip antennas and for the radiation patterns, including the backside radiation characteristics.

II. THEORETICAL OUTLINE

The formulation of a finite size microstrip structure as shown in Fig. 1 using the volume equivalent integral equation technique follows the considerations presented in [8].

For the metallic areas the boundary condition to impose is zero tangent electric field, namely:

$$\bar{E}_t^{(\text{tot})} = [\bar{E}_t^{(\text{exc})} + \bar{E}_t^{(\text{scat})}] \Big|_{S_e} = 0 \quad (1)$$

In above equation, $\bar{E}_t^{(\text{exc})}$ is the exciting electric field, which represents the excitation of the microstrip structure of Fig. 1. In this work the circuit is excited with a coaxial probe, and a delta gap excitation model as described in [9], [10] is used. In addition, $\bar{E}_t^{(\text{scat})}$ is the scattered field, which for the microstrip structure of Fig. 1 is due to both polarization currents on the dielectric and surface currents on the metallic areas:

$$\bar{E}_t^{(\text{scat})} = \int_{V_p} \bar{G}_{E_J} \cdot \bar{J}_p \, dV' + \int_{S_e} \bar{G}_{E_J} \cdot \bar{J}_s \, dS' \quad (2)$$

where \bar{G}_{E_J} is the generic electric field Green's function produced by an electric current, J_p are the polarization currents defined on the volume of the dielectric objects, and J_s are the surface currents induced on the metallic areas of the structure. In the present work, the mixed potential Green's functions are used instead of the field Green's functions in order to reduce the singular behavior [11]. Furthermore, in the dielectric region the volume equivalent imposes the following restriction on the total electric field:

$$\bar{J}_p = j \omega (\epsilon - \epsilon_0) \bar{E}_t^{(\text{tot})} \Big|_{V_p} \quad (3)$$

If we use the delta gap excitation model [9], [10], the exciting electric field $\bar{E}_t^{(\text{exc})}$ only exist at the connector position contacting the exciting coaxial probe, and therefore it is zero inside the dielectric. Using (1) we can then reduce (3) as follows

$$\bar{J}_p = j \omega (\epsilon - \epsilon_0) \bar{E}_t^{(\text{scat})} \Big|_{V_p} \quad (4)$$

Combining now equations (1), (2) and (4), the following system of coupled integral equations are easily obtained:

$$\bar{E}_t^{(\text{exc})} = \left\{ - \int_{V_p} \bar{G}_{E_J} \cdot \bar{J}_p \, dV' - \int_{S_e} \bar{G}_{E_J} \cdot \bar{J}_s \, dS' \right\}_{S_e} \quad (5a)$$

$$0 = \left\{ \frac{\bar{J}_p}{j \omega (\epsilon - \epsilon_0)} - \int_{V_p} \bar{G}_{E_J} \cdot \bar{J}_p \, dV' - \int_{S_e} \bar{G}_{E_J} \cdot \bar{J}_s \, dS' \right\}_{V_p} \quad (5b)$$

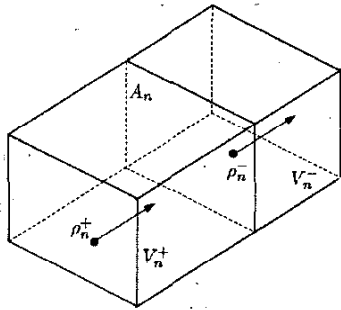
the solution of this system of integral equations gives the unknown polarization currents inside the dielectrics \bar{J}_p and induced surface currents on the metallic areas \bar{J}_s . Once known, the electromagnetic fields in the structure can be easily recovered with (2).

III. NUMERICAL IMPLEMENTATION

For the numerical solution of (5), the surface of the metallic areas are always discretized using rooftop basis and testing functions. This has been shown to be by far the best choice for representing the induced currents on the printed metallic areas of microstrip structures [11]. In the present work, this selection has proven to lead to accurate results when obtaining the scattering parameters and input impedances of printed microstrip circuits.

For the discretization of the finite dielectric objects, a first choice has been presented in [8]. In this case a combination of pulse basis functions with deltas for testing is selected. This formulation leads to a matrix system which is not symmetrical, since the testing procedure on the surface of the metallic areas is performed in a different way as the testing in the dielectric volume. In particular, when the base is taken in the metallic areas and the testing in the dielectric, the gradient of the electric scalar potential Green's function can not be avoided. In this case the reaction integrals contain a singularity of the order of $(1/r^3)$, which can not be extracted easily with numerical procedures. To avoid the singularity, the testing using deltas is applied to the center point of the volume cell. The advantage of doing so is that the testing point never lies inside the base integration, therefore avoiding the singularity of the Green's function. However, if the thickness of the dielectric substrate is electrically very small, then a Green's function exhibiting fast variations must be integrated, since then the testing point lies very close to the base integration. For the examples shown in this paper (substrate thickness $t < 0.0001 \lambda$), as many as 240 points were needed in the surface integration of the metallic printed areas in order to treat conveniently this quasi-singular situation. When the thickness of the substrate increases up to ($t > 0.01\lambda$), then only 24 points are needed to achieve a similar degree of accuracy.

To overcome this limitation, a novel numerical treatment of the finite dielectric objects has been implemented. In this case a full Galerkin approach employing rooftop functions inside the dielectric objects is formulated (see



$$\bar{f}_n(\bar{r}') = \begin{cases} \frac{A_n}{V_n^-} \rho_n^+ & , \bar{r}' \text{ en } B_n^+ \\ \frac{A_n}{V_n^+} \rho_n^- & , \bar{r}' \text{ en } B_n^- \\ 0 & , \text{Otherwise} \end{cases}$$

$$\nabla \cdot \bar{f}_n(\bar{r}') = \begin{cases} +\frac{A_n}{V_n^-} & , \bar{r}' \text{ en } B_n^+ \\ -\frac{A_n}{V_n^+} & , \bar{r}' \text{ en } B_n^- \\ 0 & , \text{Otherwise} \end{cases}$$

Fig. 2. Basis functions defined in two contiguous volume brick cells.

Fig. 2 for the definition of the basis and testing functions). The first advantage of this technique is that it produces a fully symmetrical triaxial system. In addition, for all the interactions the gradient of the electric scalar potential is transferred to the testing function, resulting in a constant charge defined inside the volume of the brick cell used for the discretization of the geometry. Consequently, the evaluation of all the reaction integrals requires the treatment of weak singularities of the type $(1/r)$. In the present work these weak singularities are treated numerically following simple procedures. The singular surface integrals are evaluated using polar coordinates, since the Jacobean of the polar transformation exactly compensate the weak singularity of the Green's functions. Following the same idea, the volume singular integrals are evaluated using spherical coordinates. In this case the Jacobean of the transformation is (r^2) , which completely annihilate the weak $(1/r)$ singularity of the Green's functions. The total function to be integrated behaves very smoothly, thus requiring only 64 points for each volume integral to achieve convergence, even for very small substrate thickness.

IV. RESULTS

The efficient numerical implementation of the volume equivalent integral equation technique derived in this paper has allowed for the first time to evaluate precisely the input impedance and radiation characteristics of finite microstrip antennas.

The first structure investigated is the microstrip patch antenna presented in [8] (Fig. 3). However [8] does not give results on the input impedance of the antenna, and in [8] the radiation patterns obtained with a volume equivalent and with a surface equivalent formulation do not agree well, therefore indicating the presence of inaccuracies. In Fig. 4 we present for the first time the input impedance of this antenna. The figure shows the results obtained with the two approaches developed in this paper and the results obtained with a spatial domain multilayered Green's functions infinite dielectric model [11]. It can be seen that in this case the three techniques agree very well, and in particular a radiation resonance appears at 1.875 GHz. The radiation patterns of this structure at the resonant frequency are shown in Fig. 5a (E-plane) and Fig. 5b (H-plane). The figures only show the results obtained with

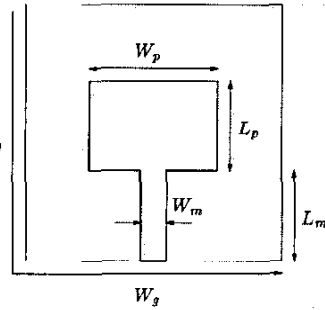


Fig. 3. Printed patch antenna introduced in [8]. The dimensions are $L_g = 15.0\text{cm}$, $W_g = 15.0\text{cm}$, $L_p = 5.0\text{cm}$, $W_p = 5.0\text{cm}$, $L_m = 5.0\text{cm}$, $W_m = 1.0\text{cm}$. The dielectric permittivity is $\epsilon_r = 2.56$ and the thickness $h = 0.2\text{cm}$.

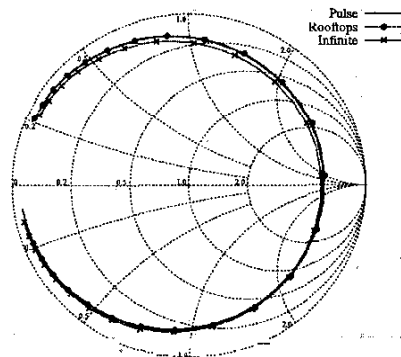


Fig. 4. Input impedance of the antenna presented in [8].

rooftop in the substrate since the results obtained with pulses are very similar. The figures also show the results obtained with the infinite substrate model, and the results presented in [8]. The radiation patterns are similar in all cases in the upper half space, but not in the lower half space. In particular, with the infinite substrate model there is no information about the radiation patterns in the backside region.

In order to verify the results obtained with the new numerical implementation of the volume equivalent integral equation, a second microstrip patch antenna presented in

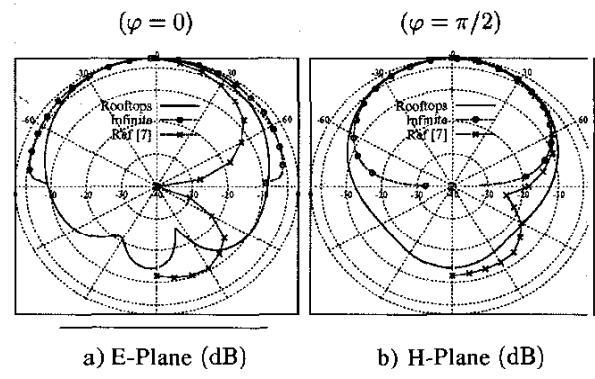


Fig. 5. Radiation patterns of the antenna presented in [8].

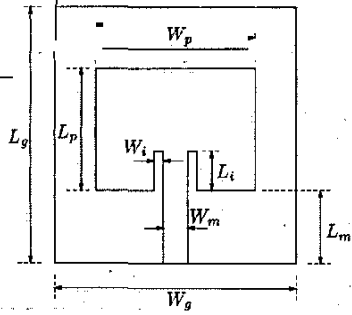


Fig. 6. Printed patch antenna introduced in [12]. The dimensions are $L_g = 40.0\text{mm}$, $W_g = 40.0\text{mm}$, $L_p = 15.70\text{mm}$, $W_p = 24.0\text{mm}$, $L_m = 13.0\text{mm}$, $W_m = 4.90\text{mm}$, $L_i = 3.30\text{mm}$, $W_i = 0.55\text{mm}$. The dielectric permittivity of the substrate is $\epsilon_r = 2.33$, and the thickness $h = 1.57\text{mm}$.

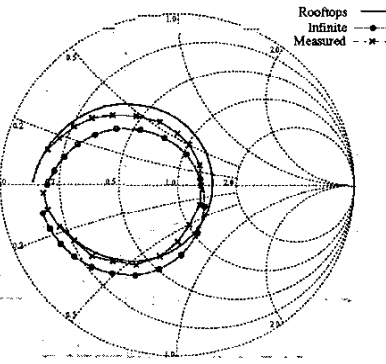


Fig. 7. Input impedance of the structure shown in Fig. 6.

[12] is studied (Fig. 6). First, we present in Fig. 7 the input impedance of this antenna, and we compare the results with data obtained from measurements. Also the results obtained with the infinite dielectric model are included for reference. It can be seen that in all cases the results are good, but the input impedance obtained with the new finite dielectric model is closer to measurements than the infinite dielectric model. In this case, then, it is important to take into account the side effects of the finite size dielectric substrate if accurate results are desired.

Finally, we present the radiation patterns of this structure at 5.94 GHz in Fig. 8a (E-plane) and Fig. 8b (H-plane). The figures compare the results obtained with the new approach, with the infinite substrate results, and with measurements. It can be seen that the agreement is good, and in particular the backside radiation predicted by the new numerical model is very closed to the real measured radiation patterns.

V. CONCLUSIONS

In this paper we have presented two efficient numerical implementations of the volume equivalent integral equation technique. The new models have been applied to the calculation of the electrical characteristics of finite size microstrip structures. Both the input impedance of microstrip patch antennas and the radiation patterns are in good agreement as compared to measurements. The new

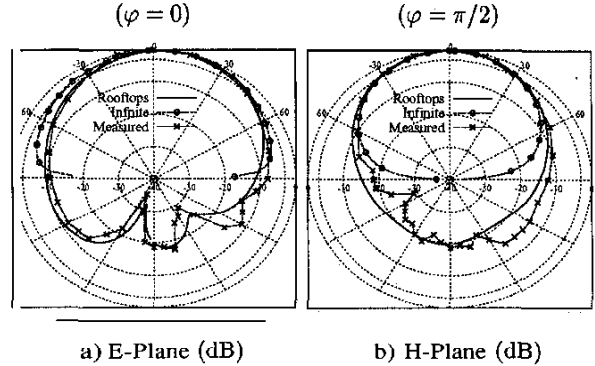


Fig. 8. Radiation patterns of the antenna shown in Fig. 6.

technique can be used for the design of microstrip circuits with reduced volume, and for the prediction of the backside radiation of real practical microstrip antennas.

REFERENCES

- [1] Q. Chaudhry, R. Alidio, G. Sakamoto, and T. Cisco, "A SiGe MMIC variable gain cascode amplifier," *IEEE Microwave and Wireless Components Letters*, vol. 12, pp. 424–428, November 2002.
- [2] F. Mesa and R. Marques, "Integral representation of spatial green's function and spectral domain analysis of leaky covered strip-like lines," *IEEE Transactions on Microwave Theory and Techniques*, vol. 43, pp. 828–837, April 1995.
- [3] N. Kinayman and M. I. Aksun, "Efficient use of closed form green's functions for the analysis of planar geometries with vertical connections," *IEEE Transactions on Microwave Theory and Techniques*, vol. 45, pp. 593–603, May 1997.
- [4] J. R. Mosig and F. E. Gardiol, *A Dynamic Radiation Model for Microstrip Structures*, ch. 3, pp. 139–237. Academic Press, 1982.
- [5] P. Gay-Balmaz and J. R. Mosig, "Three dimensional planar radiating structures in stratified media," *Int J Microwave and Millimeter Wave Computer Aided Engineering*, pp. 330–343, July 1997.
- [6] M. I. Aksun and G. Dural, "Comparative evaluation of absorbing boundary conditions using green's functions for layered media," *IEEE Transactions on Antennas and Propagation*, vol. 44, pp. 152–156, February 1996.
- [7] T. K. Sarkar and E. Arvas, "An integral equation approach to the analysis of finite microstrip antennas: Volumen/surface formulation," *IEEE Transactions on Antennas and Propagation*, vol. 38, pp. 305–312, March 1990.
- [8] T. K. Sarkar, S. M. Rao, and A. R. Djordjevic, "Electromagnetic scattering and radiation from finite microstrip structures," *IEEE Transactions on Microwave Theory and Techniques*, vol. 38, pp. 1568–1575, November 1990.
- [9] G. V. Eleftheriades and J. R. Mosig, "On the network characterization of planar passive circuits using the method of moments," *IEEE Transactions on Microwave Theory and Techniques*, vol. 44, pp. 438–445, March 1996.
- [10] A. A. Melcon, J. R. Mosig, and M. Guglielmi, "Efficient CAD of boxed microwave circuits based on arbitrary rectangular elements," *IEEE Transactions on Microwave Theory and Techniques*, vol. 47, pp. 1045–1058, July 1999.
- [11] J. R. Mosig, "Arbitrarily shaped microstrip structures and their analysis with a mixed potential integral equation," *IEEE Transactions on Microwave Theory and Techniques*, vol. 36, pp. 314–323, February 1988.
- [12] F. Tiezzi, A. A. Melcon, and J. R. Mosig, "A new excitation model for microstrip antennas on finite size ground planes," in *Proceedings of IEEE, AP-2000 Symposium, AP-S, 2000*, 1A9, No. 0277.